Scilight

Environmental and Microbial Technology

https://www.sciltp.com/journals/emt

Article

Decoding the Prolonged Suppression of Zn on Fermentative Hydrogen Generation from Sewage Sludge

Xiaomin Li [1,2,†], Mingyang Liu [1,†], Francesco Secundo [3], Chen Lyu [2] and Yanan Yin [1,*]

[1] Institute of Nuclear and New Energy Technology (INET), Tsinghua University, Beijing 100084, China
[2] Key Laboratory of Songliao Aquatic Environment Ministry of Education, School of Municipal and Environmental Engineering, Jilin Jianzhu University, Changchun 130118, China
[3] Istituto di Scienze e Tecnologie Chimiche "Giulio Natta", Consiglio Nazionale delle Ricerche via Mario Bianco 9, 20131 Milan, Italy
* Correspondence: yinyn@mail.tsinghua.edu.cn
† These authors contributed equally to this work.

How To Cite: Li, X.; Liu, M.; Secundo, F.; et al. Decoding the Prolonged Suppression of Zn on Fermentative Hydrogen Generation from Sewage Sludge. *Environmental and Microbial Technology* **2026**, *1*(1), 7.

Received: 3 December 2025
Revised: 8 January 2026
Accepted: 12 January 2026
Published: 20 January 2026

Abstract: The presence of zinc (Zn) in various wastes poses significant challenges to biohydrogen recovery from organic wastes. The inhibitory effect of Zn on hydrogen production from sewage sludge was investigated, and a pronounced inhibition on hydrogen production was observed across the tested Zn concentration range (200–2000 mg/L). With the increase of Zn dosage from 200 mg/L to 500 mg/L, cumulative hydrogen production (hydrogen yield) decreased from 39 mL (73.5 mL/g SCOD) to 8 mL (15.1 mL/g SCOD), corresponding to the increased inhibition rate from 23.5% to 84.3%. When the Zn dosage was further increased to 1000–2000 mg/L, hydrogen production dropped to less than 5 mL (9.42 mL/g SCOD), corresponding to the inhibition rate of over 90%. With the removal of Zn stress, hydrogen-producing capacity in all groups were recovered, and the recovery rate exhibited an increasing trend with the increase of Zn dosage. Microbial-community analysis revealed that Zn addition markedly suppressed hydrogen-producing genera such as *Enterococcus* and *Clostridium_sensu_stricto_14*. After stress removal, the system partially reconstituted its hydrogen-producing ability by enriching Zn-tolerant functional genera like *Pseudomonas, Acinetobacter* and *Clostridium_sensu_stricto_13.* Metabolic analysis revealed that Zn inhibited hydrogen production by suppressing glucose decomposing and ferredoxin-related hydrogen-producing pathways, and formate decomposition served as the main hydrogen-producing pathway in the presence of Zn stress. After stress removal, glucose decomposing and ferredoxin-related hydrogen-producing pathways replaced formate-decomposing pathway as the hydrogen-producing pathways. This study exhibited a long-term response of microorganisms to Zn inhibition, and provided a theoretical basis for understanding the metabolic mechanism of Zn inhibition on hydrogen production from actual organic waste.

Keywords: biohydrogen; Zn inhibition; sewage sludge; dark fermentation; recovery; metabolic analysis

1. Introduction

Hydrogen is considered one of the most promising fuel candidates due to its high calorific value (142 MJ/kg) and clean combustion products [1]. With its high energy density and environmentally friendly byproducts, hydrogen (H_2) is an ideal energy carrier to replace fossil fuels. As the demand for a low-carbon society grows, sustainable hydrogen production technologies have gained significant attention [2,3]. Biological technologies are

developed for the mild reaction conditions and high environmental benefits, and dark fermentation is considered the most applicable biological way for its high hydrogen production rate and easy operation [4,5]. In addition, dark fermentation has exhibited great potential in turning organic wastes into hydrogen, thus achieving benefits in both energy field and environment area [1,6].

However, due to the complex composition of organic wastes, there are many challenges to achieve an efficient hydrogen production from actual organic wastes [5]. For example, the recalcitrant organics restricts the biological degradation process, the inherent inhibitors may be toxic to hydrogen-producing microorganisms and fail the fermentation system, etc. [7,8]. Among various inhibitors, heavy metals have exhibited more complex impact: trace metal elements are crucial for microbial growth and metabolism, proper concentration of metal elements could stimulate the metabolic activity [8–11], while excessive metal elements may be toxic to microorganisms, thereby inhibiting the dark fermentation hydrogen production process [12,13].

Sewage sludge has exhibited a good potential as a substrate for hydrogen production for its high organic content, large amount and readily available fermentation facilities in wastewater treatment plant. As the main byproduct generated during wastewater treatment, residual sludge usually contains various heavy metals, which pose great impact on hydrogen production performance. Among various heavy metals, heavy metal Zn is widely present in wastewater. With the enrichment of wastewater treatment in residual sludge, the concentration of Zn in residual sludge ranges from 42.1 to 3568.3 mg/kg [14], and can even reach as high as 30,000 mg/kg in some Zn-rich sludge [15]. As one of the essential metals for microbial metabolism, moderate Zn can enhance fermentation performance, while excessive concentration can inhibit microbial metabolic activity and even lead to microbial death [16]. Previous studies have investigated the effect of Zn on hydrogen production during anaerobic fermentation. The results showed that the inhibition threshold of Zn fluctuated widely in different fermentation systems. Specifically, when sucrose was used as a substrate, the inhibition threshold of Zn inhibition was 1–40 mg/L [17,18]. In the dairy wastewater system, inhibition occurred when Zn concentration was 10–400 mg/L [9]. When glucose was used as substrate, the inhibitory concentration was further increased to 500–2000 mg/L [19,20]. When granular sludge was utilized to produce hydrogen from sucrose containing wastewater, the inhibition threshold reached 1000–5000 mg/L [21]. Due to differences in substrate, inoculum and operating conditions, the inhibition threshold of Zn varied significantly between 1 mg/L and 1000 mg/L [9,17–21]. Currently, research on the impact of Zn on hydrogen production primarily focuses on short-term effects, typically within 48–72 h [18,22,23], while the information about long-term response of microorganisms after a high-concentration Zn shock is limited, especially for hydrogen production from actual organic wastes. In addition, in-depth mechanistic research from the perspective of biological metabolism is still lacking.

This study aimed to investigate the effect of Zn on hydrogen production from sewage sludge. An 80-h inhibition experiment was conducted to determine the Zn inhibition threshold in the sludge fermentation system. Following this, an 80-h recovery experiment was performed after Zn removal to explore the long-term microbial response to Zn inhibition. Volatile fatty acids (VFAs), the evolution of microbial community structure, and the abundances of functional enzymes were examined to reveal the intrinsic working mechanism of Zn impacts. The research results will deepen the understanding of the Zn impacts on fermentative hydrogen production, providing reference for optimizing the hydrogen production performance from actual organic wastes.

2. Materials and Methods

2.1. Substrate and Inoculum

The sewage sludge was collected from the secondary sedimentation tank of a municipal sewage treatment plant in Beijing, China. The total solids (TS), volatile solids (VS), and pH values of sewage sludge were 42.6 ± 1.6 g/L, 24.6 ± 1.1 g/L, and 6.7 ± 0.2, respectively. Before being used as a substrate, sewage sludge was pretreated in a high-pressure reactor at 121 ℃ for 30 min. After pretreatment, the soluble chemical oxygen demand (SCOD) and pH value of sewage sludge were 5.9 g/L and 6.5 ± 0.2, respectively. Pretreated sludge was filtered through qualitative filter paper (rapid flow) and the supernatant of the heat-treated sewage sludge was collected, and stored at 4 ℃ until being used as substrate.

Digested sludge collected from the primary digestion tank of the urban sewage treatment plant was used as the inoculation source. The TS and VS of digested sludge were 47.8 ± 2.4 g/L and 22.8 ± 1.2 g/L, respectively. Before inoculation, the collected sludge was boiled for 30 min to inhibit the methanogens [24].

2.2. Experimental Design

This experiment was composed of inhibition sets and a recovery sets. For the inhibition sets, flasks with working volume of 100 mL were used, 90 mL collected sludge supernatant was used as substrate and 10 mL

pretreated digested sludge was used as inoculum. Based on the reported Zn thresholds [9,20,21], Zn dosage of 200–2000 mg/L (200, 500, 1000, 1500, and 2000 mg/L) was adopted in this study, and $ZnCl_2$ was used as Zn source. Experimental set without Zn addition was set as control group. Initial pH of all experimental sets were adjusted to be 7.0 ± 0.1 with 0.1 mol /L NaOH and HCl, and nitrogen gas was flushed for 5 min to remove residual oxygen. Then, sealed flasks were placed in a water bath shaker at 36 ℃ and 120 rpm. The experiments were performed until the termination of hydrogen production. Each experiment was conducted in triplicate.

The recovery sets were performed after the inhibition sets. By the termination of inhibition sets, mixtures in different fermentation groups were centrifuged to collect the microorganisms, and the microorganisms were washed by normal saline for 3 times to wash off the residual Zn. Then, the washed microorganisms were inoculated in fresh sludge supernatant that was prepared from pretreated sludge. Working volume of the recovery sets was 100 mL, containing 90 mL sludge supernatant and 10 mL microorganisms that was washed and re-suspended. Then, pH of all sets were adjusted to be 7.0 ± 0.1 with 0.1 mol /L NaOH and HCl, and nitrogen gas was flushed for 5 min to remove residual oxygen. Then, sealed flasks were placed in a water bath shaker at 36 ℃ and 120 rpm. Each experiment was conducted in triplicate.

2.3. Analytical Methods

TS and VS were determined according to the standard method of the American Public Health Association (APHA, 1995). Volume of biogas was measured by water displacement method. A gas chromatograph (model 112A, Shanghai, China) equipped with a thermal conductivity detector (TCD) was used to analyse the content of hydrogen in biogas. Gas volumes were normalized to standard temperature and pressure. For hydrogen analysis, a gas chromatograph (model 112A, Shanghai, China) equipped with a thermal conductivity detector (TCD) and a TDX-01 packed column (3 m long, 3 mm in diameter) was used. The column, detector, and injector temperatures were set to 160 °C, 110 °C, and 180 °C, respectively. Argon was used as the carrier gas, and the pre-column pressure was set at 0.2 MPa. All gas production data were converted to standard conditions (0 °C, 760 mm Hg). Polysaccharides were determined using the phenol sulfate method, and protein was measured using Lowry method. For the analysis of VFAs and alcohols, an HP 7890 gas chromatograph (Agilent, Santa Clara, CA, USA) equipped with a flame ionization detector (FID) and a DB-FFAP column was used. A 0.8 μL sample was injected, and the column flow rate was 2.2 mL/min (helium). The inlet temperature was set at 160 °C with a split ratio of 15:1. The oven temperature was initially set to 80 °C for 1 min, then increased to 230 °C at a rate of 15°C/min, with the detector temperature set to 250 °C. Before analysis, all liquid-phase parameters were filtered through a 0.45 μm membrane to ensure sample purity and analytical accuracy. In order to analyse the kinetic model of the hydrogen production process, a modified Gompertz model was applied [25]:

$$H = P \cdot \exp\{-\exp[Rm \cdot e(\lambda - t)/P + 1]\}$$

The meanings of parameters H, t, P, R_m, and λ in the model are cumulative hydrogen production (mL), reaction time (h), hydrogen production potential (mL), maximum hydrogen production rate (mL/h), and lag time (h).

After each fermentation stage, microbial samples were collected and analyzed using high-throughput sequencing. Detailed analysis conditions can refer to Yin and Wang [26]. Microbial samples were labeled according to the Zn dosage. For example, the fermentation group with a Zn dosage of 0 mg/L for the inhibition set was labeled as I_0. Fermentation group for recovery set with a Zn dosage of 200 mg/L was labeled as R_200.

This experiment employed principal component analysis (PCA) to analyse the beta diversity of microbial communities and visualized the results using a two-dimensional scatter plot. Bray curtis was adopted as the distance algorithm based on genus level. Additionally, dbRDA was used to analyze the relationship between environmental factors and microbial community structure. dbRDA allows for the simultaneous display of the relationships between samples, environmental factors, and microorganisms, helping to identify key environmental drivers influencing sample distribution, as well as key species associated with environmental changes. Correlation heatmap analysis was performed to calculate the correlation coefficients between dominant microorganisms and environmental factors, revealing the relationships between microbes and environmental factors. Spearman was adopted as the relative coefficient. PICRUSt was adopted to elucidate the abundance of functional enzymes involved in hydrogen production process. Hydrogen-producing metabolism pathways was constructed based on the Kyoto Encyclopedia of Genes and Genomes (KEGG) database and obtained the abundance of related functional genes by comparing with the MetaCyc database [27,28].

3. Results

3.1. Inhibitory Effect of Zn on Fermentation Process

For the inhibition sets, the results showed that the produced biogas was only composed of hydrogen and carbon dioxide, methane was not detected. Different Zn dosages had significant impacts on the fermentation performance (Figure 1). Zn played an important regulatory role in hydrogen production during anaerobic fermentation, and its impact varied significantly along with different dosages [29]. As shown in Figure 1A, the control group without Zn addition exhibited specific hydrogen production capacity, with a maximum cumulative hydrogen production of 51 mL and hydrogen yield of 96.05 mL/g SCOD. The addition of 200 mg/L Zn inhibited hydrogen production by 23.5% compared to the control group, resulted in a maximum cumulative hydrogen production of 39 mL and hydrogen yield of 73.5 mL/g SCOD. When the Zn dosage was further increased to 500–2000 mg/L, hydrogen production was severely inhibited, with cumulative hydrogen production dropped to 4–8 mL and hydrogen yield decreased to 7.53–15.1 mL/g SCOD. The inhibition rates exceeded 84.3% (Figure 1B). These results exhibited substantial toxicity of Zn to hydrogen-producing microorganisms, resulted in significant inhibition to hydrogen production. The inhibition rate of hydrogen production increased with the increase of Zn dosage. It is important to note that, in addition to Zn^{2+}, $ZnCl_2$ also introduces chloride ions (Cl^-) into the system, which may potentially affect microbial activity due to its impact on ionic strength. The Cl^- concentration range corresponding to the $ZnCl_2$ concentrations used in this study was 217–2170 mg/L. Previous studies have shown that microbial activity can be maintained when chloride ion concentrations are below 9250 mg/L [30]. Therefore, the inhibition of hydrogen production observed in this study was mainly contributed by Zn ions.

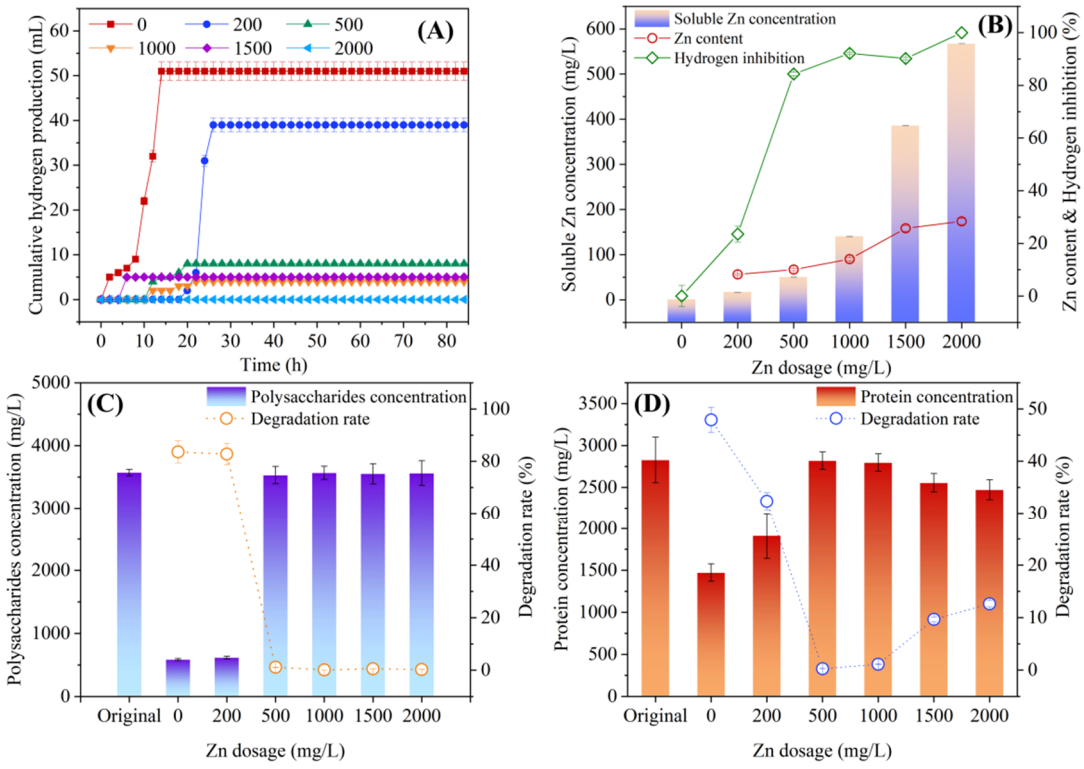

Figure 1. The effect of Zn concentration on hydrogen production is as follows: (**A**) the variation of hydrogen production over time; (**B**) Dissolved Zn concentration and hydrogen production inhibition rate; (**C**) Polysaccharide concentration and degradation rate; (**D**) Protein concentration and degradation rate.

The inhibitory impact of Zn observed in this study exhibited great variance comparing with the system adopted glucose as substrate [19], which demonstrated a significant higher tolerance to Zn inhibition at lower Zn concentrations. In the system performing hydrogen production from glucose, hydrogen production was stimulated by 75% in the presence of 200 mg/L Zn, and the inhibition rate of 67.5% was observed when Zn dosage reached 500 mg/L. However, when Zn dosage was increased to 1000–1500 mg/L, hydrogen production was completely inhibited in glucose system, but remained active in this study, implied the better tolerance of sewage sludge system to high Zn concentrations. Both studies observed complete hydrogen production inhibition in the presence of 2000

mg/L Zn. This difference may be attributed to the complex composition of sludge. From one side, organic matter, solid particles and other components in sewage sludge may alter the bioavailability of Zn through binding or adsorption, thus relieving the inhibitory effect of Zn; on the other side, some other coexisting inhibitory factors in the system may synergistically amplify the toxic effects of Zn. Both sides contributed to the more complex impact of Zn on hydrogen production from sewage sludge.

Kinetic analysis of the hydrogen production process was performed to obtain the hydrogen production potential, lag time and maximum hydrogen production rate (Table 1). Typically, the addition of heavy metals can prolong the lag time (λ) of hydrogen generation. Previous studies have shown that the lag time increased with the increase of metal concentration [21]. A similar initial trend was also observed in this study. As shown in Table 1, with the addition of Zn, the lag time was significantly prolonged from 7 h to approximately 22 h when Zn dosage was 200 mg/L. This is because in the presence of 200 mg/L Zn, more time is needed for hydrogen-producing microorganisms to adapt. However, contrary to the general rule mentioned above, with the further increase of Zn dosage to 500–2000 mg/L, lag time exhibited decreased trend, implied the more complex inhibiting mechanism of Zn in sewage sludge fermentation system.

Table 1. Kinetic analysis of hydrogen production in different fermentation groups.

Zn Dosage		H (mL)	λ (h)	R_m (mL/h)	R^2
0	inhibition	51.1	6.9	7.18	0.9895
	recovery	66.1	3.5	11.70	0.9999
200	inhibition	39.0	21.7	14.28	0.9874
	recovery	42.0	27.0	10.75	0.9999
500	inhibition	8.0	9.0	0.86	0.9822
	recovery	5.5	30.0	0.41	0.8770
1000	inhibition	4.0	9.0	0.34	0.9799
	recovery	6.0	0	0.85	0.9085
1500	inhibition	5.0	4.9	13.57	0.9999
	recovery	8.0	0	1.07	0.9600
2000	inhibition	/	/	/	/
	recovery	2.0	0.8	4.54	0.9999

The impact of Zn on hydrogen-producing lag time also varied in different studies. In studies using sucrose as a substrate, the lag time was extended from 4.6 h to 29.9 h when the Zn dosage increased from 0 to 5000 mg/L [21]. However, in studies using glucose as a substrate, 200 mg/L Zn shortened the lag time and promoted hydrogen production [19], further proved the significant impact of substrate type on Zn toxicity expression. Similarly, other heavy metal ions showed different impact on the lag time. In different substrate systems, the effects of nickel (Ni) and lead (Pb) also show similar trends: when using brewery wastewater as the substrate, the increase of the concentration of Ni oxide nanoparticles to 20 mg/L prolongs the lag time to 13 h [31]. When using waste-activated sludge as a substrate, adding 5 mg/L Ni^{2+} extended the lag time of the control group from 2.03 h to 20.39 h [32]. When organic portion of urban solid waste was used as substrate, the lag time was increased from 12.5 ± 2.8 h to 23.8 ± 2.8 h with the increase of Pb concentration from 0 to 100 mg/L [33]. These comparisons indicated that although most heavy metals consistently prolonged the lag time, Zn exhibited a more complex impact pattern under different concentrations and substrate conditions. This provided important clues for further elucidating the specific inhibitory mechanism of Zn on hydrogen production performance.

Dissolved Zn in the liquid phase in the fermentation system was examined. It can be seen that Zn concentration in the liquid phase was significantly lower than the added Zn dosage (Figure 1B). Due to the high complexity of the sludge system, externally added Zn could be quickly fixed through various pathways, including adsorption on microbial cell surfaces, precipitation with sulfides or phosphates in the sludge, and complex reactions with organic components such as extracellular polymers [34]. Specific data showed that in the control group without added Zn, the concentration of dissolved Zn was under detection. In the experimental group with a Zn dosage of 200 mg/L, the dissolved Zn concentration was only 16 mg/L, accounted for 8.22% of the total dosage. With the increase of Zn dosage, the absolute concentration of dissolved Zn increased, and its proportion in the total amount gradually increased to 30%. This may be due to the saturation of adsorption sites. Similar phenomena were also reported in studies exploring other heavy metals. The study explore the influence of iron (Fe) on sludge fermentation, the actual measured Fe^{2+} concentration in the liquid phase was significantly lower than the addition. This was mainly due to the complex composition of the sludge, and the added Fe^{2+} could be consumed through various pathways, including adsorption on sludge particles, precipitation, and oxidation [35]. In the co-fermentation system of algae and different pretreated sludges, a large amount of Fe^{2+} was lost during the

fermentation process due to oxidation and precipitation. The monitoring data of residual Fe^{2+} in the liquid phase of the system showed that, under the condition of Fe^{2+} dosage of 0–1000 mg/L, the concentration of residual Fe^{2+} in the liquid phase ranged from 8.75 mg/L to 324.65 mg/L, and exhibited an upward trend with the increase of dosage [36]. Similar phenomenon was also observed for copper (Cu): when Cu dosage was in the range of 0–1000 mg/L, most of the added Cu was separated from the liquid phase. With the increase of Cu dosage, soluble Cu content also showed an upward trend [34].

When using complex organic waste as substrate for anaerobic fermentation, polysaccharides are typical carbon source for microbial metabolism [34]. The degradation efficiency of polysaccharides had a significant impact on hydrogen production, as they constituted the primary available carbon source in the process [37]. The addition of Zn significantly affected the degradation behaviour of polysaccharides. As shown in Figure 1C, the initial polysaccharide concentration in the substrate was 3570 mg/L. In the control group, polysaccharide concentration decreased to 585 mg/L by the end of the reaction, achieved a degradation rate of 83%. With the addition of 200 mg/L Zn, although hydrogen production was inhibited by 23.5%, the degradation rate of polysaccharides still reached 82.9%, which was essentially equivalent to that of the control group. This phenomenon of "high degradation, low hydrogen production" indicates that, at this concentration, the inhibitory effect of Zn mainly occurs during the acidification stage, rather than the hydrolysis process. Microorganisms might reorganize the carbon flow and electrons produced from polysaccharide degradation to maintain cellular homeostasis and other life activities instead of producing hydrogen. In addition, the active performance on substrate degradation indicated that microorganisms remained active, Zn only induced the change of metabolic pathways. When the Zn concentration was further increased to 500–2000 mg/L, the polysaccharide degradation rate sharply decreased to less than 1%, indicating the excessive concentrations of Zn had severely inhibited the overall metabolic activity of microorganisms.

Protein is an important nitrogen and carbon source, could directly participate in anaerobic metabolism. Besides, during the fermentation, extracellular polymeric substances (EPS) can be formed and contribute to protein content in liquid phase. In addition, with the death and division of microbial cells, intra-cellular protein could be released to liquid phase. Therefore, the concentration of soluble proteins in the system is the balance between their release and consumption by microorganisms [19]. In this study, soluble proteins were derived from both the substrate itself and the release of inoculated microorganisms. As shown in Figure 1D, the initial concentration of soluble protein in the substrate was 2827 mg/L. In the control group, protein concentration decreased to 1472 mg/L (47.9%). Instead, in the presence of 200 mg/L Zn, protein concentration after reaction was 1914 mg/L (decrease value of 32.3%), indicating that 200 mg/L Zn posed significantly impact on the release and utilization of proteins by microorganisms. When Zn dosage was further increased to 500 mg/L, protein degradation was only 0.3%.

The observed trend of protein degradation was consistent with the study which explored the effect of ZnO nanomaterials on protein degradation in anaerobic fermentation systems [38]. Although protein degradation was strongly inhibited when the Zn concentration increased to 500 mg/L, the degradation rate was still positive, indicating that the metabolic function of the microbial system was not completely lost and that the microbial community structure might remain relatively intact. When Zn dosage was further increased up to 2000 mg/L, the protein degradation rate showed an inevitable rebound, reaching 12.6% at 2000 mg/L Zn. This change might be due to adaptive adjustments in the structure and function of the microbial community, with some tolerant bacterial groups gradually gaining dominance and restoring limited metabolic capacity.

Throughout the entire reaction process, the protein degradation rate remained positive. This phenomenon suggested that the inhibitory effect of Zn on microorganisms was likely functional and reversible, rather than irreversible and due to cellular structural damage, as also validated through subsequent recovery experiments.

3.2. Recovery Test of Fermentation Performance after Zn Removal

3.2.1. Recovery of Hydrogen Production

During the recovery stage, the generated biogas consisted only of hydrogen and carbon dioxide, with no methane detected. This indicated that throughout the entire recovery process, the metabolic type of the fermentation system remained dominated by hydrogen production, and the activity of methane bacteria was effectively inhibited. The hydrogen production along with time in the recovery experiment are shown in Figure 2A. After replacing the fresh culture medium, microorganisms in different Zn dosage groups exhibited a recovery of hydrogen-producing activity; however, significant differences were observed in the degree of recovery and start-up speed. The microorganisms in the 200 mg/L Zn group resumed hydrogen production after 26 h and reached a peak within the following 6 h, with a cumulative hydrogen production of 42 mL and hydrogen yield of 79.1 mL/g SCOD. However, the 500 mg/L Zn group began to recover after 32 h and only reached 6 mL of cumulative

hydrogen production, and hydrogen yield of 11.3 mL/g SCOD after 4 h. It is worth noting that the 1000–2000 mg/L Zn group exhibited hydrogen production activity in the early stages of the recovery period (2 h), exhibited shorter lag time than other groups, which might be related to the accelerated initiation of basal metabolic activities by microorganisms to maintain survival under high Zn stress.

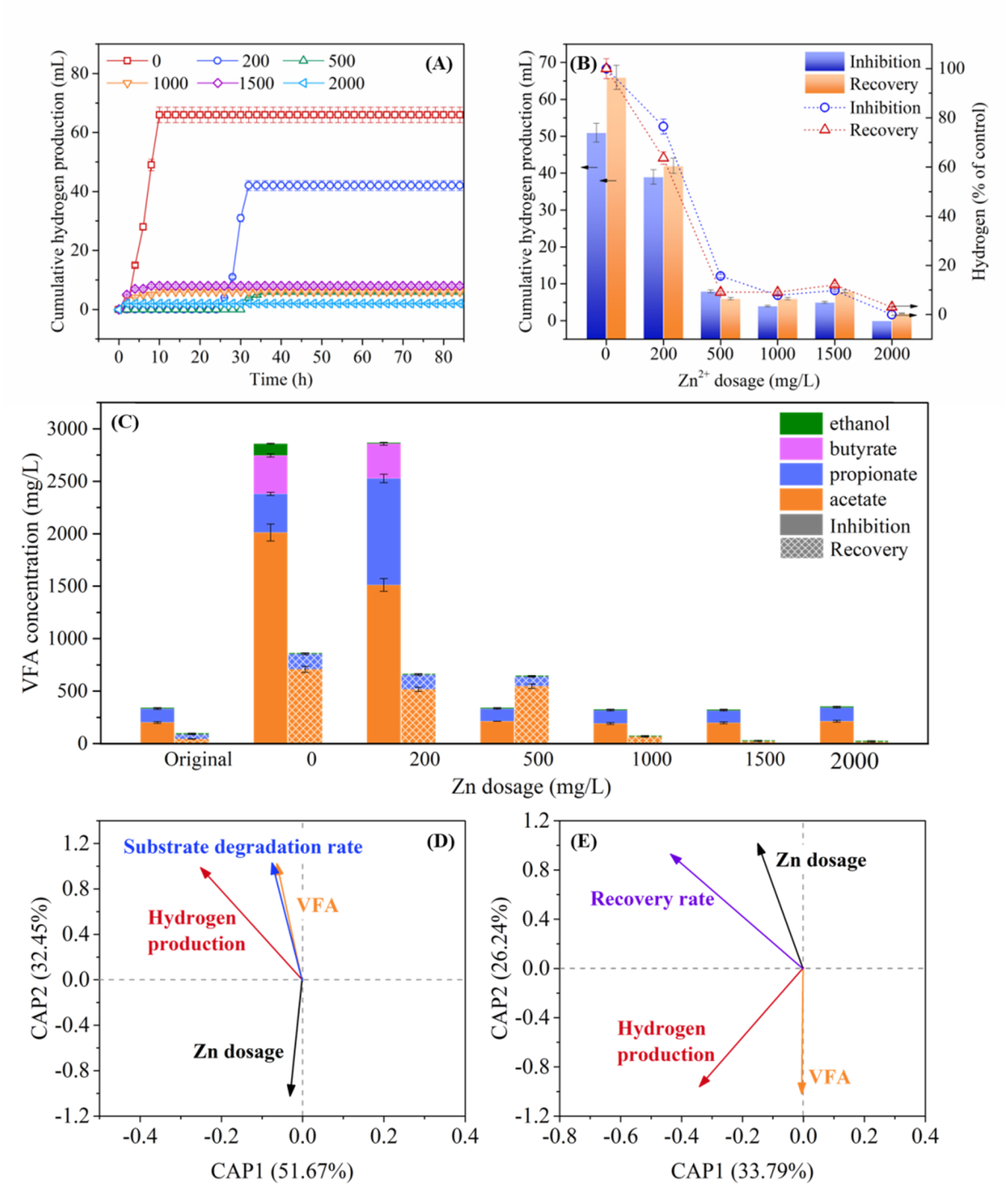

Figure 2. (**A**) Hydrogen production over time during the recovery experiment; (**B**) Accumulated hydrogen production and hydrogen production efficiency under inhibition and recovery.; (**C**) VFA in different concentrations of Zn after fermentation; (**D**,**E**) Correlations among Zn dosage, VFA, and fermentation groups revealed by db-RDA analysis.

Further comparison of the hydrogen production performance between the inhibition experiment and the recovery experiment is shown in Figure 2B and Table 1, revealed that the control group maintained high hydrogen production and efficiency in both inhibition and recovery experiments, and hydrogen production in the recovery experiment was further strengthened, indicated that after the first round of fermentation, hydrogen-producing microorganisms were enriched and remained highly active, with their metabolic potential fully released after

obtaining fresh nutrients. In the recovery group of 200 mg/L Zn, hydrogen production was only 63.6% of that in the control group, which was even lower than the hydrogen production in inhibition group (76.5%). Similarly, in the recovery group of 500 mg/L Zn, hydrogen production was only 9% of that in the control group and 15.7% lower than the inhibition group. This indicated that under lower Zn concentration conditions, the recovery experiment did not show metabolic recovery advantages, and its inhibition rate was higher than that of the inhibition group, suggesting the persistent inhibitory effect of Zn on hydrogen-producing microorganisms. In contrast, in the recovery group of 1000–2000 mg/L Zn, the recovery groups showed advantage in hydrogen production than the inhibition groups. Further demonstrated the reversibility of high-dose Zn in inhibiting microorganisms.

Although the hydrogen production in the recovery experiment did not return to the control group level, there was a significant increase in cumulative hydrogen production compared to the inhibition stage. This "incomplete recovery" phenomenon was consistent with the recovery patterns of microbial metabolic functions under various environmental stresses. For example, in a fermentation hydrogen production system using glucose as a substrate, the hydrogen production capacity of microorganisms could be partially restored at Zn concentrations of 500–2000 mg/L, and the recovery kinetics trend was highly consistent with the results obtained in this study [19]. Similarly, in the study of the inhibitory mechanism of free organic acids on hydrogenotrophic methanogens, *Methanobacterium formalicum* was found to restore methane activity when the concentration of free acetic acid was below 0.97 g/L, but irreversible inhibition occurred beyond this threshold. Similarly, under the stress of propionic acid and butyrate, the specific methanogenic activity of hydrogenotrophic methanogens could not be fully restored even at concentrations higher than 0.69 g/L and 0.61 g/L, respectively [39,40]. The different recovery performance indicated the different microbial response to inhibition stress in different fermentation systems.

By comparing the fermentation performance of inhibition and recovery processes, it can be seen that although Zn had a significant inhibitory effect on the hydrogen production process, this inhibition was not achieved by completely inactivating the microorganisms. Under high Zn stress, a certain number of microorganisms can maintain their survival through various adaptive mechanisms. This may be due to the unique cell membrane structure or ion transport system of certain microorganisms, which enables them to resist the toxicity of high Zn concentrations or adapt to harsh environments by regulating their gene expression and altering their metabolic pathways. Therefore, the presence of Zn mainly inhibited the process of hydrogen production, rather than directly killing all microorganisms involved in fermentation. In the recovery experiment, the microbial community demonstrated strong adaptability after the Zn was washed away from the system. Over time, microorganisms gradually adapted to the altered nutritional environment resulting from the removal of Zn. They gradually restored their hydrogen production capacity by adjusting the metabolic network, reactivating the expression of suppressed genes related to hydrogen production, and restoring the activity of key enzymes involved in this process [19].

In the system with glucose as the sole substrate [19], the recovery degree of hydrogen production capacity was significantly better than in the system with sludge cracking solution as the substrate. This difference might be due to several reasons: firstly, the composition of the sewage sludge was complex, and other inhibitory substances or competitive microorganisms might remain active in the presence of Zn, which continuously interfered with the recovery of hydrogen-producing communities. Secondly, glucose, as a easily degradable carbon source, could provide energy and carbon sources to microorganisms more quickly and efficiently, promoting the recovery of their metabolic activity. The low availability of organic components in the sludge cracking solution might limit the growth and metabolism of microorganisms during the recovery period. Additionally, microbial communities exposed to complex substrates for an extended period may undergo structural changes, resulting in lower functional redundancy and resilience compared to those cultured on a single substrate. This discovery further emphasized the important role of substrate composition on microbial stress resistance and functional recovery. It provided a theoretical basis for optimizing the stability and impact resistance of actual organic waste in hydrogen production systems.

3.2.2. Recovery of VFAs Formation

In the anaerobic fermentation process, the production of hydrogen was usually accompanied with volatile fatty acids (VFAs) formation. VFAs composition is an important indicator for evaluating the characteristics of fermentation processes [41,42]. Figure 2C showed the concentration changes of VFAs in the fermentation system with different Zn dosages. Acetic acid, as the main fermentation product, was considered one of the most effective hydrogen-producing metabolic types [43]. Butyrate was also a typical liquid end product of hydrogen production by some obligate anaerobic bacteria [44,45]. The more acetic acid and butyrate produced, the more hydrogen gas was produced. Before fermentation, VFAs present in the substrate were mainly composed of acetic acid and

propionic acid. In the inhibition experiment, the total amount of VFAs produced in the control group was 2860 mg/L, comprised acetic acid of 2012 mg/L, propionic acid of 368 mg/L, butyrate of 365 mg/L, and ethanol of 113 mg/L. The proportion of acetic acid was 70.3 %, indicating that the metabolism of the control group was dominated by the acetic acid type fermentation. In the group with 200 mg/L Zn, the total amount of VFAs remained basically unchanged. However, its composition underwent significant changes: the acetic acid content decreased to 1512 mg/L, the propionic acid content increased, the butyrate remained stable, and the ethanol content decreased significantly. Fermentation type favorable for hydrogen production (acetic-type) was inhibited, and the fermentation type unfavorable for hydrogen production (propionic-type) was strengthened, contributed to the impaired hydrogen production in the group with 200 mg/L Zn.

When the Zn dosage was further increased to 500–2000 mg/L, the total amount of VFAs sharply decreased to approximately 350 mg/L, primarily consisted of acetic acid and propionic acid, indicating that high concentrations of Zn severely inhibited the overall acidification process. This phenomenon was consistent with existing research: in the study of hydrogen production from glucose, it was mentioned that 500–2000mg/L Zn inhibited acid production activity, resulted in a significant decrease in VFAs production from 2839 mg/L to 100–200 mg/L [19]. In the recovery experiment, the total amount of VFAs in the 0–500 mg/L Zn group was restored to about 700 mg/L, still mainly composed of acetic acid, accompanied by a small amount of propionic acid, and the hydrogen production capacity was correspondingly restored to a certain extent. In the 1000–2000 mg/L Zn group, the ability of microorganisms to generate VFAs was still weak, and the level of hydrogen recovery was limited. Throughout the entire inhibition recovery experiment, acetic acid fermentation consistently dominated [34]. Therefore, by regulating the Zn concentration, it was possible to achieve targeted guidance of the fermentation pathway, thereby optimizing the yield distribution of volatile fatty acids and hydrogen gas.

3.2.3. Correlations among Vital Factors at Different Fermentation Stages

The relationship between environmental factors and microbial community structure was further analyzed through dbRDA. Various environmental factors were represented by arrows, and the angle between the arrows reflected the correlation between variables: variables pointing in similar directions had a positive correlation. In contrast, those pointing in opposite directions had a negative correlation [19]. Figure 3D showed the correlation between Zn dosage, substrate degradation rate, VFAs, and hydrogen production. The results showed that Zn dosage was significantly negatively correlated with substrate degradation rate, VFAs, and hydrogen production, indicating that with an increase of Zn dosage, the hydrolysis and acidification processes, as well as hydrogen production metabolism were all significantly inhibited. There was a significant positive correlation between substrate degradation rate, VFAs, and hydrogen production, indicating that these metabolic processes were synergistic. The increase in substrate degradation rate induced the generation of VFAs. At the same time, the accumulation of VFAs especially when acetic acid and butyrate were the primary products, was typically accompanied with higher hydrogen production, forming a positive coupling in metabolism. Figure 3E further illustrated the relationship between dominant factors in the recovery stage. There was a positive correlation between Zn dosage and recovery rate; that is, the higher the Zn dosage, the more significant the recovery of the metabolic activity after removing Zn stress. This phenomenon might be due to the more potent initial inhibition of microbial communities caused by high Zn stress. After the stress was relieved, the surviving tolerant bacterial community or metabolic potential could be more fully expressed, thereby exhibiting higher relative recovery potential. At the same time, Zn dosage was still negatively correlated with VFAs and hydrogen production, further confirmed the sustained inhibitory effect of Zn on VFAs and hydrogen metabolism. The above correlation was highly consistent with the trend observed in the research of Zn inhibition on hydrogen production from glucose, indicating that the inhibition and recovery laws of Zn on anaerobic fermentation systems had certain universality in different substrates and systems.

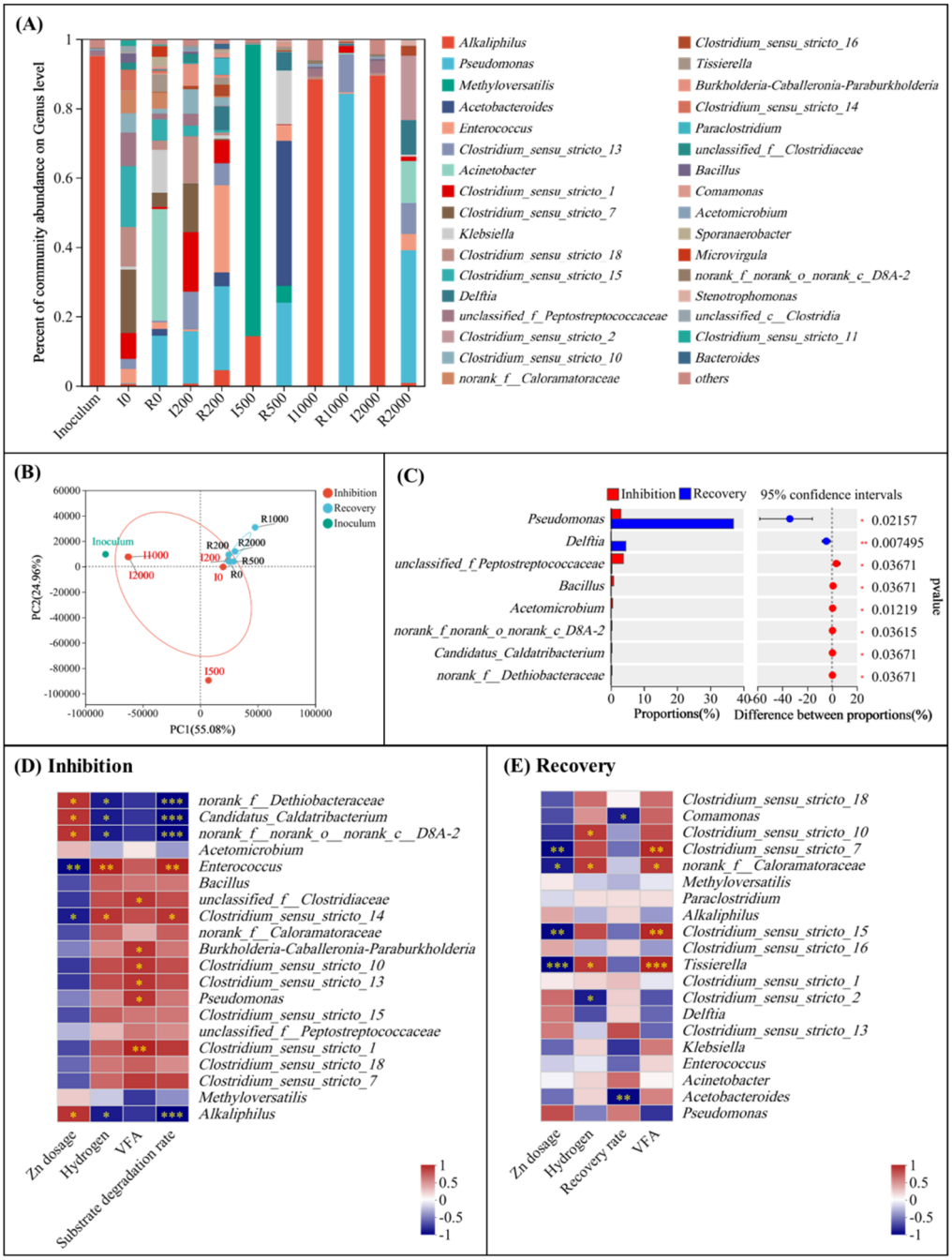

Figure 3. (**A**) Horizontal distribution of microorganisms; (**B**) PCA of different concentrations of Zn in the inhibited group and recovery group; (**C**) Genera was significantly affected by Zn dosage; (**D**) Correlations between the dominant genera and fermentation characteristics during Inhibition; (**E**) Correlations between the dominant genera and fermentation characteristics during Recovery. * represents $0.01 < p \leq 0.05$, ** represents $0.001 < p \leq 0.01$, *** represents $p < 0.001$.

3.3. Variance of Microbial Distribution at Different Fermentation Stages

Figure 4A showed the microbial composition (genus level) under different Zn stress at different fermentation stages. In the inoculum, *Alkaliphilus* was the main genus, accounted for 95%. After the fermentation reaction in the control group, the microorganisms was mainly consisted of *Clostridium_sensu_stricto_7* (18.3%), *Clostridium_sensu_stricto_15* (17.5%), *Clostridium_sensu_stricto_18* (11.4%), *unclassified_f__Peptostreptococcaceae* (9.7%), *Clostridium_sensu_stricto_1* (7.4%), all other bacterial genera were below 7%. *Clostridium* was considered the primary hydrogen-producing bacterium in various fermentation environments [46,47]. Studies have reported that *Clostridium* became dominant after dark fermentation showed a strong correlation with hydrogen production [1,48,49]. Hydrogen production from sludge fermentation in other studies also demonstrated high abundance of *Clostridium* [49]. The main microorganisms in the control group of

the recovery experiment were changed to *Acinetobacter* (32.1%), *Pseudomonas* (14.4%), *Klebsiella* (12.4%), and *Clostridium_sensu_stricto_15* (6.1%). The rest were all below 6%. *Acinetobacter* was a hydrolysis and acid-producing microorganism widely present in fermentation systems with complex organic substrates [34,50]. Its enrichment was related to the accumulation of propionates. *Pseudomonas* has been shown to contribute to the aggregation of hydrogen-producing microorganisms, as confirmed in the literature. This strain could turn proteins and carbohydrates into acetate, accompany with hydrogen production [51–55]. *Klebsiella* [56] and *Clostridium* [46] were both hydrogen-producing bacteria, contributed to hydrogen production in recovery experiments. In the 200mg/L Zn inhibition group, *Clostridium* still accounted for a high abundance. At the same time, *Pseudomonas* (14.4%) was enriched, contributed to the aggregation of hydrogen-producing microorganisms [51–55]. Therefore, the system maintained hydrogen-producing activity However, although the total abundance of hydrogen-producing bacteria did not show significant changes, the addition of Zn still led to a decrease in hydrogen production, indicating that it might directly inhibit hydrogen production by affecting microbial metabolic activity rather than population structure. In the recovery experiment, the abundance of *Enterococcus* increased to 25.1%. *Enterococcus* was a facultative anaerobic, Gram-positive, non-motile, and spore-forming bacterium that could produce hydrogen [57,58]. After removing Zn stress, *Enterococcus* was significantly enriched, indicating that it could not compete with Zn-tolerant bacteria due to toxicity inhibition in the presence of Zn. Once the inhibition was relieved, *Enterococcus* quickly occupied the vacant ecological niche due to its rapid growth ability. Although the hydrogen production increased compared to the inhibition group at this concentration, the overall hydrogen production capacity of the system was not fully recover to the level of control group. When the Zn concentration reached 500 mg/L, the community structure underwent significant changes, and the microorganisms primarily consisted of *Methylloversatilis* (84.1%) and *Alkaliphilus* (14.3%). *Methyloversatilis* belongs to acid-producing bacteria and contributed to VFAs production [59]. *Alkaliphilus* was an acid-producing bacterium associated with the proteins degradation. It can grow in seawater salt concentrations up to 33 g/L and produce hydrogen sulfide as the primary gas product in the presence of sulfides, resulting in severe inhibition to hydrogen production process [60]. After relieving Zn stress, *Acetobacter* (41.8%) and *Klebsiella* (15.5%) became the dominant genera, and *Klebsiella* had been confirmed to be hydrogen-producing bacteria [61]. Therefore, their hydrogen production ability was partially restored at this stage. When Zn dosage further increased to high stress conditions of 1000–2000 mg/L, the microbial community structure tended to simplify, dominated by *Alkaliphilus*, and its composition was most similar to that of the inoculum. At this time, microbial activity was weak or even inactive, and the system had essentially lost its ability to produce hydrogen. The microbial community did not undergo significant changes during the fermentation process, further verified the inhibition of microbial growth and metabolism by high concentration. After relieving Zn stress, the community was dominated by *Pseudomonas* and supplemented by *Clostridium*, both of which belonged to hydrogen-producing bacteria. However, due to the metabolic function changes of microorganisms under high-concentration Zn stress, even if hydrogen-producing bacteria were enriched, hydrogen production ability was limited recovered. Comparing with other heavy metals such as Cu and Ni, the toxic effect of Zn on microorganisms was more manifested as reversible metabolic inhibition rather than irreversible cell damage. Microorganisms can adapt to Zn stress through changes in population structure and adjustments in metabolic function, and subsequently restore partial biological activity after stress relief. This provided a new theoretical perspective for understanding the adaptive response of microorganisms to heavy metal stress and the long-term stability of fermentation hydrogen production systems.

Principal Component Analysis (PCA) is an effective method for analyzing beta diversity in microbial communities, which can visually display the differences in community structure between different samples. As shown in Figure 4B, based on the PCA analysis results, all samples could be clearly divided into three main clusters, indicating a significant impact of Zn concentration on microbial community composition. In the inhibition experiment, the control groups were located in the fourth quadrant. Samples with 200 mg/L Zn were clustered in the third quadrant. When the Zn concentration increased to 500 mg/L, the sample position shifted to the first quadrant. The sample with 1000–2000 mg/L Zn were concentrated in the second quadrant, in the same quadrant as the inoculum. This result further confirmed that the microbial community structure was closest to the inoculum at this high Zn concentration, and no significant changes had occurred. The above distribution pattern indicated that Zn concentration was a key environmental factor driving the evolution of microbial community structure, and there was a significant difference in community composition between different Zn concentration treatment groups in the inhibition experiment. In the recovery experiment, all samples under Zn stress (0–2000 mg/L) were clustered in the first quadrant. Compared with the inhibition experiment, the PCA results from the recovery experiment were more concentrated, indicating that after relieving Zn inhibition, the microbial community structures of the different treatment groups tended to be similar, and the differences between communities were significantly reduced. Compared to the initial inoculum, significant differences in community structure persisted in the recovery

experiment. The microorganisms in the inoculum were scattered and would form new dominant microbial communities under certain fermentation conditions, indicating that the fermentation was effective and the microorganisms were active. This further suggested that Zn stress did not cause irreversible community collapse.

By comparing and analysing the microbial communities in the inhibition and recovery experiments, several species that showed significant differences under Zn stress and removal conditions were identified. At the species level, Zn was a key environmental factor driving changes in microbial distribution and composition, as shown in Figure 4C. *Pseudomonas* and *Delftia* were significantly enriched in the recovery experiment, indicating that although they were initially inhibited, they were still able to recover. In a dormant state in the presence of Zn, they could quickly resume growth and reproduction after Zn was removed. Research has shown that a particular concentration of Zn could induce *Pseudomonas* to synthesise specific enzyme proteins or stress factors, thereby endowing it with the ability to resist Zn stress [62]. *Delftia* was resistant to various heavy metal ions and could alleviate heavy metal toxicity by secreting extracellular polymeric substances (EPS) that facilitated adsorption and complexation, promoted metal precipitation, and participated in nanoscale metal transformation mechanisms [63]. After relieving Zn inhibition, *Pseudomonas* and *Delftia* quickly regained their dominant bacterial communities due to their strong environmental adaptability and rapid growth characteristics. By contrast, *Bacillus, Acetomicrobium, norank_f__norank_o__norank_c__D8A-2, Candidatus_Caldatribacterium, norank_f__Dethiobacteraceae, Thermovirga, Proteiniphilum,* and groups such as *norank_f__norank_o__norank_c__norank_p__Firmicutes* were able to maintain a particular abundance under Zn inhibition conditions but were eliminated in the recovery experiment.

Correlation heatmap analysis was adopted to reveal the correlation between main environmental factors and top 20 genera. In the inhibition experiment (Figure 4D), Zn dosage and *norank_f__Dethiobacteraceae, Candidatus_Caldatribacterium, norank_f__norank_o__norank_c__D8A-2* and *Alkaliphilus* showed a significant positive correlation, indicating that these bacterial genera had strong tolerance to Zn stress, and their abundance increased with the increase of Zn dosage. On the contrary, Zn dosage was significantly negatively correlated with *Enterococcus* and *Clostridium*, indicating that these two bacterial genera were more sensitive to Zn and their growth and metabolic activities were efficiently inhibited by Zn [64]. Hydrogen was significantly negatively correlated with the aforementioned Zn tolerant bacterial genera (*norank_f__Dethiobacteraceae, Candidatus_Caldatribacterium, norank_f__norank_o norank_cD8A-2, Alkalihilus*), indicating that these groups did not possess or only had weak hydrogen production capabilities. It showed a significant positive correlation with *Enterococcus* and *Clostridium-sensu-stricto_14*, which served as the main hydrogen-producing bacteria in this fermentation system [48]. Among them, *Clostridium sensu stricto 14* was the most important hydrogen-producing group within *Clostridium*, further confirmed the close relationship between hydrogen production and *Clostridium* species. The accumulation of VFAs showed a significant positive correlation with *unclassified_Clostridiaceae, Burkholderia-Caballeronia-Paraburkholderia, Clostridium_sensu_stricto_10, Clostridium_sensu_stricto_13, Pseudomonas,* and *Clostridium-sensu-stricto_1*, indicating that these genera played a key role in the acidification process and highlighted their critical contribution to VFAs production, a pattern consistent with previous studies [65–67]. The substrate degradation rate was significantly negatively correlated with the Zn tolerant bacterial genera (*norank_f__Dethiobacteraceae, Candidatus_Caldatribacteria, norank_f__norank_o norank_cD8A-2, Alkalihilus*), and significantly positively correlated with the hydrogen producing bacterial genera *Enterococcus* and *Clostridium_sensu_stricto_14*. The trend of substrate degradation rate was highly consistent with that of hydrogen. It was opposite to the effect of Zn dosage: as the Zn dosage increased, the abundance of Zn-tolerant groups increased. At the same time, the substrate degradation rate and hydrogen production both decreased. Conversely, when the Zn dosage was low, hydrogen-producing bacteria dominated, exhibiting higher substrate degradation rates and hydrogen production. This result, confirmed from the perspective of community ecology, suggests that Zn primarily regulates the metabolic function and product distribution of the system by screening for Zn-tolerant and Zn-sensitive groups.

In the recovery experiment, correlation analysis further revealed the complex relationship between the residual effects of Zn stress and microbial functional recovery (Figure 4E). Zn dosage showed a significant negative correlation with *Clostridium_sensu_stricto_7, norank_f__Caloramatoraceae, Clostridium_sensu_stricto_15* and *Tissierella*, indicating that these genera are highly sensitive to Zn stress. The damage they suffered during the inhibition stage increased with the increase in Zn concentration, resulting in a continuous decrease in their abundance during the recovery experiment. At the same time, the above-mentioned bacterial genera were significantly positively correlated with VFA content. Combined with the phenomenon of generally low VFA total in the recovery experiment shown in Figure 2C, it can be inferred that high concentrations of Zn caused irreversible or difficult-to-repair damage to these acid-producing bacteria, thereby limiting the recovery of the overall acidification capacity of the system. Hydrogen was significantly positively correlated with

Clostridium-sensu-stricto_10, norank_f__Caloramatoraceae, and *Tissierella*, indicating that these bacterial genera were key groups in promoting the recovery of hydrogen production function. However, there was a significant negative correlation between hydrogen production and *Clostridium_sensu-stricto_2*, indicating that although both species/genera were *Clostridium*, there was differentiation in functional expression during the recovery process. Some groups may undergo metabolic pathway changes or lose their hydrogen production capacity due to Zn stress, which is one reason why the hydrogen production performance of the system has not been fully restored to its initial level. The recovery rate was significantly negatively correlated with *Comamonas* and *Acetobacter*. Based on Figure 3A, it could be further observed that after washing away 200 mg/L and 500 mg/L Zn, the abundance of these two bacterial genera significantly increased, inhibiting the recovery of other functional bacterial groups or their own metabolic direction, which was not conducive to hydrogen production. Ultimately, this led to the overall recovery effect of washing away Zn within this concentration range, failing to reach the expected level.

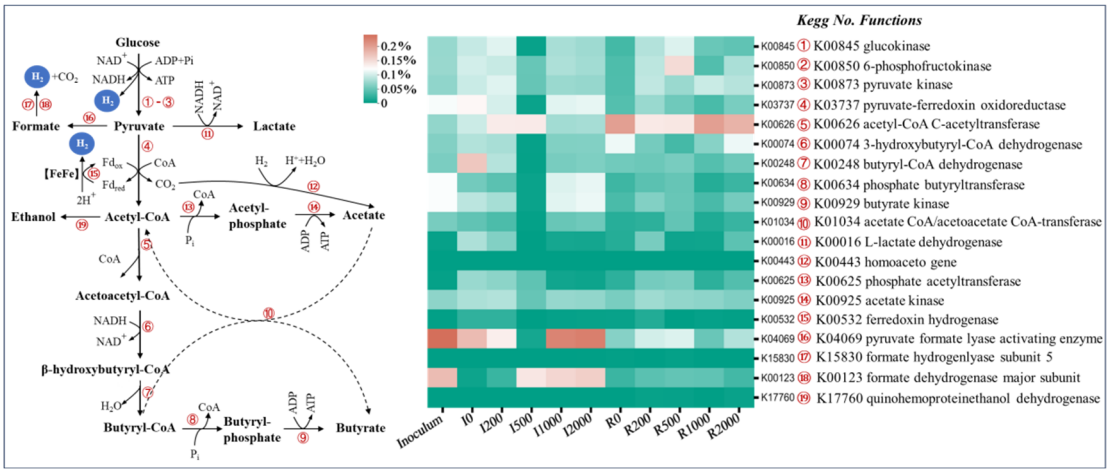

Figure 4. Analysis of key enzymes involved in hydrogen production.

3.4. Analysis of Key Enzymes Involved in Hydrogen Production

Figure 4 showed the abundances of key functional genes related to hydrogen production. The functional genes directly involved in hydrogen production included K00845, K00850, and K00873 (No.1–3), which were key enzymes in the process of glucose degradation; K00532 (No.15) was ferredoxin hydrogenase, a core catalytic unit responsible for electron transfer and proton reduction to generate hydrogen gas; K15830 and K00123 (No.17–18) were involved in the hydrogen production pathway through formate decomposition. In addition to the metabolic processes that promoted hydrogen production mentioned above, some competitive or hydrogen-consuming metabolic pathways also had a significant impact on net hydrogen production. For example, K00016 (No.11) promoted lactate production, while the expression of K00443 (No.12) led to the reduction of hydrogen and carbon dioxide to produce acetate, thus consuming hydrogen gas [68]. In addition, K17760 (No.19) could promote the generation of ethanol, further divert carbon sources, and reduce hydrogen production potential.

During the inhibition experiment, the control group exhibited the highest abundances of K00845, K00850, and K00873 (No.1–3). Meanwhile, K00532 (No.15) and K00123 (No.18) also maintained a particular high abundance, jointly ensuring the good performance in hydrogen production. In addition, the increase in abundance of K04069 (No.16) promoted the formation of formate. In contrast, the increase in abundance of K00248 (No.7) was beneficial for the synthesis of butyrate, which was consistent with the trend of increasing butyrate content in Figure 2C. When 200 mg/L Zn was added, the abundance of K00845, K00850, and K00873 (No.1–3) showed an upward trend and remained the main hydrogen-producing pathway; At the same time, the abundance of K00123 (No.18) increased, indicating that the pathway of formate dehydrogenase catalyzing the decomposition of formate into hydrogen and carbon dioxide was enhanced, thereby maintained hydrogen production to a certain extent. On the other hand, the increase in abundance of K00626 (No.5) might interfere with the normal metabolism of acetyl-CoA by promoting its conversion to acetyl-CoA, thereby inhibiting hydrogen synthesis. Previous studies had shown that this pathway could inhibit hydrogen production by disrupting the formation of acetyl-CoA and enhancing its oxidation process [69]. When 500 mg/L Zn was added, the abundances of K00845, K00850, K00873 (No.1–3) and K00532 (No.15) all decreased, indicating significant inhibition of the glucose decomposition hydrogen production pathway and the ferredoxin hydrogenase pathway. At this point, the abundance of K00123 (No.18) further increased, and formate decomposition became the main hydrogen production pathway. However,

the hydrogen production capacity of this pathway was limited, resulting in a decrease in overall hydrogen production. Meanwhile, K00626 (No.5) maintained a high abundance and continued to inhibit hydrogen synthesis. When Zn dosage was further increased to 1000–2000 mg/L, there was no significant difference in the abundance of all detected genes compared to the initial state of the inoculum, indicating that microbial metabolic activity was basically stagnant, and hydrogen and acid production processes were almost completely stopped.

In the recovery experiment, key functional genes related to hydrogen metabolism, K00845, K00850, K00873 (No.1–3), K00532 (No.15), and K00123 (No.18), were all restored to a certain abundance level after removing Zn stress of 200–2000 mg/L. Among them, the abundance of K00845, K00850, and K00873 (No.1–3) was relatively high, indicating that the glucose decomposition hydrogen production pathway became the dominant hydrogen production mechanism during the recovery stage. At the same time, an increase in the abundance of K00626 (No.5), K00016 (No.11), and K17760 (No.19) was also observed in the recovery experiment. K00626 (No.5) was responsible for catalyzing the conversion of acetyl-CoA. Previous studies have shown that enhancing this metabolic branch disrupts the normal metabolic flow of acetyl-CoA and promotes its oxidation process, thereby inhibiting hydrogen production [69]. K00016 (No.11) promoted the generation of lactate, forming a competitive metabolic shunt for the hydrogen production pathway; K17760 (No.19) promoted the synthesis of ethanol, further consuming available carbon sources. The enhancement of these competitive metabolic pathways might be one of the important reasons for the incomplete recovery of hydrogen production capacity to its initial level during the recovery phase.

4. Conclusions

This study provides valuable insights into the inhibitory effects of Zn on hydrogen production from sewage sludge. Our results indicate that Zn concentrations in the range of 200–2000 mg/L significantly suppressed hydrogen generation, with inhibition rates increased with the increase of Zn concentration. While hydrogen production was severely inhibited at higher Zn levels, microbial community analysis revealed that Zn exposure primarily affected key hydrogen-producing genera, reducing their abundance. During the recovery phase, the microbial community showed a partial restoration of hydrogen production, driven by the enrichment of Zn-tolerant genera. Metabolic pathway analysis identified that Zn hindered hydrogen production by disrupting glucose and ferredoxin-related pathways, with formate decomposition emerging as the dominant pathway under Zn stress. Upon removal of Zn, the glucose and ferredoxin pathways were recovered, underscoring the microbial system's ability to adapt. This study not only improves our understanding of the long-term microbial response to Zn stress but also contributes to optimizing strategies for hydrogen production from organic waste in environments with Zn contamination.

Author Contributions

X.L.: writing—original draft preparation, Investigation; M.L.: writing—original draft preparation, Investigation; F.S.: Formal analysis, Writing-original draft; C.L.: Funding acquisition, Conceptualization; Y.Y.: Writing—original draft, Investigation, Funding acquisition, Formal analysis. All authors have read and agreed to the published version of the manuscript.

Funding

This research was funded by Department of Science and Technology of Jilin Province (20240304089SF) and The Fundamental Research Funds for the Central Universities and China Huaneng Group Technology Project (HNKJ25LN217).

Institutional Review Board Statement

Not applicable.

Informed Consent Statement

Informed consent was obtained from all subjects involved in the study.

Data Availability Statement

Data will be made available on request.

Conflicts of Interest

Given the role as the editorial board member of *Environmental and Microbial Technology*, Yanan Yin had no involvement in the peer review of this paper and had no access to information regarding its peer-review process. Full responsibility for the editorial process of this paper was delegated to another editor of the journal.

Use of AI and AI-Assisted Technologies

During the preparation of this work, the authors used Deepseek to proofread for grammatical errors. After using this tool/service, the authors reviewed and edited the content as needed and take full responsibility for the content of the published article.

References

1. Jain, R.; Panwar, N.L.; Jain, S.K.; et al. Bio-hydrogen production through dark fermentation: An overview. *Biomass Convers. Biorefinery* **2024**, *14*, 12699–12724. https://doi.org/10.1007/s13399-022-03282-7.
2. Tian, H.; Li, J.; Yan, M.; et al. Organic waste to biohydrogen: A critical review from technological development and environmental impact analysis perspective. *Appl. Energy* **2019**, *256*, 113961. https://doi.org/10.1016/j.apenergy.2019.113961.
3. Wang, J.; Yin, Y. Fermentative hydrogen production using various biomass-based materials as feedstock. *Renew. Sustain. Energy Rev.* **2018**, 92, 284–306. https://doi.org/10.1016/j.rser.2018.04.033.
4. Das, D.; Veziroglu, T.N. Advances in biological hydrogen production processes. *Int. J. Hydrogen Energy* **2008**, *33*, 6046–6057. https://doi.org/10.1016/j.ijhydene.2008.07.098.
5. Dahiya, S.; Chatterjee, S.; Sarkar, O.; et al. Renewable hydrogen production by dark-fermentation: Current status, challenges and perspectives. *Bioresour. Technol.* **2021**, *321*, 124354. https://doi.org/10.1016/j.biortech.2020.124354.
6. Mohanakrishna, G.; Sneha, N.P.; Rafi, S.M.; et al. Dark fermentative hydrogen production: Potential of food waste as future energy needs. *Sci. Total Environ.* **2023**, *888*, 163801. https://doi.org/10.1016/j.scitotenv.2023.163801.
7. Lin, R.C.; Cheng, J.; Ding, L.K.; et al. Inhibitory effects of furan derivatives and phenolic compounds on dark hydrogen fermentation. *Bioresour. Technol.* **2015**, *196*, 250–255. https://doi.org/10.1016/j.biortech.2015.07.097.
8. Hidalgo, D.; Martín-Marroquín, J.M.; Corona, F. The role of magnetic nanoparticles in dark fermentation. *Biomass Convers. Biorefinery* **2023**, *13*, 16299–16320. https://doi.org/10.1007/s13399-023-04103-1.
9. Yu, H.Q.; Fang, H.H.P. Inhibition on acidogenesis of dairy wastewater by zinc and copper. *Environ. Technol.* **2001**, *22*, 1459–1465. https://doi.org/10.1080/09593332208618183.
10. Yang, G.; Wang, J. Various additives for improving dark fermentative hydrogen production: A review. *Renew. Sustain. Energy Rev.* **2018**, *95*, 130–146. https://doi.org/10.1016/j.rser.2018.07.029.
11. Maroušek, J. Review: Nanoparticles can change (bio)hydrogen competitiveness. *Fuel* **2022**, *328*, 125318. https://doi.org/10.1016/j.fuel.2022.125318.
12. Chen, Y.; Cheng, J.J.; Creamer, K.S. Inhibition of anaerobic digestion process: A review. *Bioresour. Technol.* **2008**, *99*, 4044–4064. https://doi.org/10.1016/j.biortech.2007.01.057.
13. Tirapanampai, C.; Intasian, P.; Uthaipaisanwong, P.; et al. Metal additives for boosting hydrogen production in anaerobic fermentation: Focus on the change of gene expression and cost analysis. *J. Clean. Prod.* **2023**, *414*, 137609. https://doi.org/10.1016/j.jclepro.2023.137609.
14. Guo, G.; Chen, T.B.; Yang, J.; et al. Regional distribution characteristics and variation of heavy metals in sewage sludge of China. *Huanjing Kexue Xuebao/Acta Sci. Circumstantiae* **2014**, *34*, 2455–2461. https://doi.org/10.13671/j.hjkxxb.2014.0619.
15. Aguilar, M.I.; Lloréns, M.; Fernández-Garrido, J.M.; et al. Heavy metals effect on the heterotrophic activity of activated sludge. *Int. J. Environ. Sci. Technol.* **2020**, *17*, 3111–3118. https://doi.org/10.1007/s13762-020-02704-1.
16. Zhang, N.; Lu, C.; Zhang, Z.; et al. Enhancing photo-fermentative biohydrogen production using different zinc salt additives. *Bioresour. Technol.* **2022**, *345*, 126561. https://doi.org/10.1016/j.biortech.2021.126561.
17. Cho, Y.; Lee, T. Variations of hydrogen production and microbial community with heavy metals during fermentative hydrogen production. *J. Ind. Eng. Chem.* **2011**, *17*, 340–345. https://doi.org/10.1016/j.jiec.2011.02.036.
18. Lin, C.-Y.; Shei, S.-H. Heavy metal effects on fermentative hydrogen production using natural mixed microflora. *Int. J. Hydrogen Energy* **2008**, *33*, 587–593. https://doi.org/10.1016/j.ijhydene.2007.09.030.
19. Lyu, C.; Li, X.; Sun, X.; et al. Inhibitory effect of zinc on fermentative hydrogen production: Insight into the long-term effect. *Int. J. Hydrogen Energy* **2024**, *110*, 63–73. https://doi.org/10.1016/j.ijhydene.2025.02.239.
20. Zheng, X.J.; Yu, H.Q. Biological hydrogen production by enriched anaerobic cultures in the presence of copper and zinc. *J. Environ. Sci. Health Part A* **2004**, *39*, 89–101. https://doi.org/10.1081/ese-120027370.
21. Li, C.; Fang, H.H.P. Inhibition of heavy metals on fermentative hydrogen production by granular sludge. *Chemosphere* **2007**, *67*, 668–673. https://doi.org/10.1016/j.chemosphere.2006.11.005.

22. Zhang, Y.; Zhao, W.; Li, S.; et al. Unraveling the mechanism of increased synthesis of hydrogen from an anaerobic fermentation by zinc ferrate nanoparticles: Mesophilic and thermophilic situations comparison. *Bioresour. Technol.* **2023**, *387*, 129617. https://doi.org/10.1016/j.biortech.2023.129617.
23. Zhang, Y.-T.; Wei, W.; Ni, B.-J. Revealing the mechanism of zinc oxide nanoparticles facilitating hydrogen production in alkaline anaerobic fermentation of waste activated sludge. *J. Clean. Prod.* **2021**, *328*, 129580. https://doi.org/10.1016/j.jclepro.2021.129580.
24. Yin, Y.; Hu, J.; Wang, J. Enriching hydrogen-producing bacteria from digested sludge by different pretreatment methods. *Int. J. Hydrogen Energy* **2014**, *39*, 13550–13556. https://doi.org/10.1016/j.ijhydene.2014.01.145.
25. Wang, J.; Wan, W. Kinetic models for fermentative hydrogen production: A review. *Int. J. Hydrogen Energy* **2009**, *34*, 3313–3323. https://doi.org/10.1016/j.ijhydene.2009.02.031.
26. Yin, Y.; Wang, J. Changes in microbial community during biohydrogen production using gamma irradiated sludge as inoculum. *Bioresour. Technol.* **2016**, *200*, 217–222. https://doi.org/10.1016/j.biortech.2015.10.027.
27. Caspi, R.; Billington, R.; Ferrer, L.; et al. The MetaCyc database of metabolic pathways and enzymes and the BioCyc collection of pathway/genome databases. *Nucleic Acids Res* **2016**, *44*, D471–D480. https://doi.org/10.1093/nar/gkv1164.
28. Park, J.-H.; Park, J.-H.; Lee, S.-H.; et al. Metabolic flux and functional potential of microbial community in an acidogenic dynamic membrane bioreactor. *Bioresour. Technol.* **2020**, *305*, 123060. https://doi.org/10.1016/j.biortech.2020.123060.
29. Zhou, Y.; Deng, H.; Wang, X.; et al. Effects of Zn^{2+} and Mn^{2+} on the photo-fermentative performance of HY01 in biohydrogen production from xylose fermentation. *Int. J. Green Energy* **2024**, *21*, 1829–1834. https://doi.org/10.1080/15435075.2023.2272850.
30. Kim, D.-H.; Kim, S.-H.; Shin, H.-S. Sodium inhibition of fermentative hydrogen production. *Int. J. Hydrogen Energy* **2009**, *34*, 3295–3304. https://doi.org/10.1016/j.ijhydene.2009.02.051.
31. Gadhe, A.; Sonawane, S.S.; Varma, M.N. Influence of nickel and hematite nanoparticle powder on the production of biohydrogen from complex distillery wastewater in batch fermentation. *Int. J. Hydrogen Energy* **2015**, *40*, 10734–10743. https://doi.org/10.1016/j.ijhydene.2015.05.198.
32. Chen, Y.; Yin, Y.; Wang, J. Effect of Ni^{2+} concentration on fermentative hydrogen production using waste activated sludge as substrate. *Int. J. Hydrogen Energy* **2021**, *46*, 21844–21852. https://doi.org/10.1016/j.ijhydene.2021.04.054.
33. Sharma, P.; Melkania, U. Impact of heavy metals on hydrogen production from organic fraction of municipal solid waste using co-culture of Enterobacter aerogenes and *E. coli*. *Waste Manag.* **2018**, *75*, 289–296. https://doi.org/10.1016/j.wasman.2018.02.005.
34. Gao, W.; Song, W.; Chen, Y.; et al. Effect of copper on fermentative hydrogen production from sewage sludge: Insights into working mechanisms. *Renew. Energy* **2024**, *231*, 121005. https://doi.org/10.1016/j.renene.2024.121005.
35. Yin, Y.; Wang, J. Mechanisms of enhanced hydrogen production from sewage sludge by ferrous ion: Insights into functional genes and metabolic pathways. *Bioresour. Technol.* **2021**, *321*, 124435. https://doi.org/10.1016/j.biortech.2020.124435.
36. Yin, Y.; Chen, Y.; Wang, J. Co-fermentation of sewage sludge and algae and Fe^{2+} addition for enhancing hydrogen production. *Int. J. Hydrogen Energy* **2021**, *46*, 8950–8960. https://doi.org/10.1016/j.ijhydene.2021.01.009.
37. Hallenbeck, P.C. Fermentative hydrogen production: Principles, progress, and prognosis. *Int. J. Hydrogen Energy* **2009**, *34*, 7379–7389. https://doi.org/10.1016/j.ijhydene.2008.12.080.
38. Zhang, L.; Zhang, Z.; He, X.; et al. Diminished inhibitory impact of ZnO nanoparticles on anaerobic fermentation by the presence of TiO_2 nanoparticles: Phenomenon and mechanism. *Sci. Total Environ.* **2019**, *647*, 313–322. https://doi.org/10.1016/j.scitotenv.2018.07.468.
39. Zhang, W.; Zhang, F.; Li, Y.-X.; et al. No difference in inhibition among free acids of acetate, propionate and butyrate on hydrogenotrophic methanogen of Methanobacterium formicicum. *Bioresour. Technol.* **2019**, *294*, 122237. https://doi.org/10.1016/j.biortech.2019.122237.
40. Zhang, W.; Zhang, F.; Li, Y.-X.; et al. Inhibitory effects of free propionic and butyric acids on the activities of hydrogenotrophic methanogens in mesophilic mixed culture fermentation. *Bioresour. Technol.* **2019**, *272*, 458–464. https://doi.org/10.1016/j.biortech.2018.10.076.
41. Yang, G.; Wang, J. Enhancement of biohydrogen production from grass by ferrous ion and variation of microbial community. *Fuel* **2018**, *233*, 404–411. https://doi.org/10.1016/j.fuel.2018.06.067.
42. Batista, A.P.; Moura, P.; Marques, P.A.S.S.; et al. Scenedesmus obliquus as feedstock for biohydrogen production by Enterobacter aerogenes and Clostridium butyricum. *Fuel* **2014**, *117*, 537–543. https://doi.org/10.1016/j.fuel.2013.09.077.
43. Yin, T.; Wang, W.; Guo, W.; et al. Enhanced Thermophilic Hydrogen Production by an Enriched Novel Acetic-Acid-Type Fermentative Bacterium from Inoculum Sludge with Nonheat Pretreatment. *Energy Fuels* **2024**, *38*, 8749–8761. https://doi.org/10.1021/acs.energyfuels.3c04696.
44. Atasoy, M.; Owusu-Agyeman, I.; Plaza, E.; et al. Bio-based volatile fatty acid production and recovery from waste streams: Current status and future challenges. *Bioresour. Technol.* **2018**, *268*, 773–786. https://doi.org/10.1016/j.biortech.2018.07.042.

45. Mugnai, G.; Borruso, L.; Mimmo, T.; et al. Dynamics of bacterial communities and substrate conversion during olive-mill waste dark fermentation: Prediction of the metabolic routes for hydrogen production. *Bioresour. Technol.* **2021**, *319*, 124157. https://doi.org/10.1016/j.biortech.2020.124157.
46. Vesga-Baron, A.; Etchebehere, C.; Schiappacasse, M.C.; et al. Controlled oxidation-reduction potential on dark fermentative hydrogen production from glycerol: Impacts on metabolic pathways and microbial diversity of an acidogenic sludge. *Int. J. Hydrogen Energy* **2021**, *46*, 5074–5084. https://doi.org/10.1016/j.ijhydene.2020.11.028.
47. Hung, C.-H.; Chang, Y.-T.; Chang, Y.-J. Roles of microorganisms other than Clostridium and Enterobacter in anaerobic fermentative biohydrogen production systems—A review. *Bioresour. Technol.* **2011**, *102*, 8437–8444. https://doi.org/10.1016/j.biortech.2011.02.084.
48. Yang, G.; Wang, J. Changes in microbial community structure during dark fermentative hydrogen production. *Int. J. Hydrogen Energy* **2019**, *44*, 25542–25550. https://doi.org/10.1016/j.ijhydene.2019.08.039.
49. Cho, S.-K.; Jeong, M.-W.; Choi, Y.-K.; et al. Effects of low-strength ultrasonication on dark fermentative hydrogen production: Start-up performance and microbial community analysis. *Appl. Energy* **2018**, *219*, 34–41. https://doi.org/10.1016/j.apenergy.2018.03.047.
50. Chuanchuan, D.; Yuling, L.; Penghe, Z.; et al. Study on anaerobic fermentation of waste activated sludge to produce volatile fatty acids by thermal-rhamnolipid treatment. *J. Chem. Technol. Biotechnol.* **2023**, *98*, 2168–2180. https://doi.org/10.1002/jctb.7429.
51. Hung, C.H.; Lee, K.S.; Cheng, L.H.; et al. Quantitative analysis of a high-rate hydrogen-producing microbial community in anaerobic agitated granular sludge bed bioreactors using glucose as substrate. *Appl Microbiol Biotechnol* **2007**, *75*, 693–701. https://doi.org/10.1007/s00253-007-0854-7.
52. Lin, C.-Y.; Chang, C.-C.; Hung, C.-H. Fermentative hydrogen production from starch using natural mixed cultures. *Int. J. Hydrogen Energy* **2008**, *33*, 2445–2453. https://doi.org/10.1016/j.ijhydene.2008.02.069.
53. Porwal, S.; Kumar, T.; Lal, S.; et al. Hydrogen and polyhydroxybutyrate producing abilities of microbes from diverse habitats by dark fermentative process. *Bioresour Technol* **2008**, *99*, 5444–5451. https://doi.org/10.1016/j.biortech.2007.11.011.
54. Guo, L.; Li, X.-M.; Zeng, G.-M.; et al. Effective hydrogen production using waste sludge and its filtrate. *Energy* **2010**, *35*, 3557–3562. https://doi.org/10.1016/j.energy.2010.04.005.
55. Xiao, B.; Liu, J. Biological hydrogen production from sterilized sewage sludge by anaerobic self-fermentation. *J. Hazard. Mater.* **2009**, *168*, 163–167. https://doi.org/10.1016/j.jhazmat.2009.02.008.
56. Maintinguer, S.I.; Fernandes, B.S.; Duarte, I.C.S.; et al. Fermentative hydrogen production with xylose by Clostridium and Klebsiella species in anaerobic batch reactors. *Int. J. Hydrogen Energy* **2011**, *36*, 13508–13517. https://doi.org/10.1016/j.ijhydene.2011.07.095.
57. Li, Y.Q.; Gu, C.T. Enterococcus pingfangensis sp. nov., Enterococcus dongliensis sp. nov., Enterococcus hulanensis sp. nov., Enterococcus nangangensis sp. nov. and Enterococcus songbeiensis sp. nov., isolated from Chinese traditional pickle juice. *Int. J. Syst. Evol. Microbiol.* **2019**, *69*, 3191–3201. https://doi.org/10.1099/ijsem.0.003608.
58. Wang, A.; Gao, L.; Ren, N.; et al. Bio-hydrogen production from cellulose by sequential co-culture of cellulosic hydrogen bacteria of Enterococcus gallinarum G1 and Ethanoigenens harbinense B49. *Biotechnol. Lett.* **2009**, *31*, 1321–1326. https://doi.org/10.1007/s10529-009-0028-z.
59. Hou, Y.-N.; Yang, C.; Zhou, A.; et al. Microbial community response and SDS-PAGE reveal possible mechanism of waste activated sludge acidification enhanced by microaeration coupled thermophilic pretreatment. *Process Biochem.* **2018**, *64*, 1–8. https://doi.org/10.1016/j.procbio.2017.09.010.
60. Takai, K.; Moser, D.P.; Onstott, T.C.; et al. Alkaliphilus transvaalensis gen. nov., sp. nov., an extremely alkaliphilic bacterium isolated from a deep South African gold mine. *Int. J. Syst. Evol. Microbiol.* **2001**, *51*, 1245–1256. https://doi.org/10.1099/00207713-51-4-1245.
61. Hu, J.M.; Yu, L.; Huang, T.Y. Impact of Anthraquinone-2-sulfonic Acid on the MO Decolorization, Hydrogen Production and Energy Creation During Anaerobic Fermentation of Klebsiella oxytocaGS-4-08 with Sucrose. *Huan Jing Ke Xue* **2016**, *37*, 3891–3898. https://doi.org/10.13227/j.hjkx.2016.10.030.
62. Quaye, J.A.; Gadda, G. Uncovering Zn^{2+} as a cofactor of FAD-dependent Pseudomonas aeruginosa PAO1 d-2-hydroxyglutarate dehydrogenase. *J. Biol. Chem.* **2023**, *299*, 103007. https://doi.org/10.1016/j.jbc.2023.103007.
63. Huang, L.K.; Wang, G.Z.; Han, L.M.; et al. Efficiency of electroplating wastewater treatment by suspended carrier integrated with MBR technology. *Zhongguo Huanjing Kexue/China Environ. Sci.* **2018**, *38*, 2490–2497.
64. Ma, H.; Wu, M.; Liu, H.; et al. Study on enhancing sludge methanogenesis by adding acetylene black and effect on the characteristics & microbial community of anaerobic granular sludge. *RSC Adv.* **2019**, *9*, 23086–23095. https://doi.org/10.1039/C9RA03142A.
65. Zhao, W.; Jiang, H.; Dong, W.; et al. Elevated caproic acid production from one-stage anaerobic fermentation of organic waste and its selective recovery by electro-membrane process. *Bioresour. Technol.* **2024**, *399*, 130647. https://doi.org/10.1016/j.biortech.2024.130647.

66. Fanfoni, E.; Sinisgalli, E.; Fontana, A.; et al. Microbial Characterisation of a Two-Stage Anaerobic Digestion Process for Conversion of Agri-Based Feedstock in Biogas and Long-Chain Fatty Acids in a Circular Economy Framework. *Fermentation* **2024**, *10*, 293. https://doi.org/10.3390/fermentation10060293.
67. Vu, D.H.; Wainaina, S.; Taherzadeh, M.J.; et al. Production of polyhydroxyalkanoates (PHAs) by Bacillus megaterium using food waste acidogenic fermentation-derived volatile fatty acids. *Bioengineered* **2021**, *12*, 2480–2498. https://doi.org/10.1080/21655979.2021.1935524.
68. Lalman, J.A.; Chaganti, S.R.; Moon, C.; et al. Elucidating acetogenic H_2 consumption in dark fermentation using flux balance analysis. *Bioresour. Technol.* **2013**, *146*, 775–778. https://doi.org/10.1016/j.biortech.2013.07.125.
69. Yin, Y.; Song, W.; Wang, J. Inhibitory effect of acetic acid on dark-fermentative hydrogen production. *Bioresour. Technol.* **2022**, *364*, 128074. https://doi.org/10.1016/j.biortech.2022.128074.